Tropical Cyclone Intensity Increase near Australia as a Result of Climate Change

KEVIN J. E. WALSH AND BRIAN F. RYAN

CSIRO Atmospheric Research, Aspendale, Australia

(Manuscript received 21 October 1998, in final form 7 September 1999)

ABSTRACT

Idealized tropical cyclones are inserted into a regional climate model and the resulting intensity evolution of the storms is examined under current and enhanced greenhouse climates. The regional climate model is implemented over a model domain near Australia. In general, storm intensities increase under enhanced greenhouse conditions, although these increases are mostly not statistically significant. The simulated intensities are compared to theoretically derived estimates of maximum potential intensity. The theoretical estimates are mostly larger than the simulated intensities, suggesting that other factors may be limiting the intensification of the storms. Two such factors are suggested: the limited horizontal resolution of the storm simulations and the presence of vertical wind shear. Significant regression relations are demonstrated between maximum intensity of the simulated storms as predicted by sea surface temperature and vertical wind shear variations, while much weaker relationships are shown between maximum intensity and sea surface temperature alone. This suggests that dynamical influences such as vertical wind shear, which are not included in theoretical estimates of maximum potential intensity, act to restrict the development of the storm and thereby its maximum intensity.

1. Introduction

It is becoming clearer that climate change may have some effects on the mean and maximum intensities of tropical cyclones. A recent review of the topic is included in Henderson-Sellers et al. (1998). A consensus appears to be emerging that under enhanced greenhouse conditions, some increases in mean and maximum tropical cyclone intensities may conceivably be expected. Maximum tropical cyclone intensities are sometimes expressed in terms of maximum potential intensity (MPI, Emanuel 1988, 1995; Holland 1997). To estimate MPI, thermodynamic parameters are applied to the output of general circulation models (GCMs, also known as global climate models) and the resulting changes in intensities under enhanced greenhouse conditions are derived (Li 1996). A modest to moderate increase in maximum cyclone intensity of 10%–20% is suggested, although these increases are presently less than the uncertainty range of the MPI predictions for the current climate, because of inaccuracies in the methods used to estimate actual MPI and large differences in the simulations of MPI between the various GCMs.

Other techniques have been used to estimate changes in mean intensities. Knutson et al. (1998) have used a combination of GCM and regional model simulations to show that increases in maximum intensities are generally expected. In their study, 51 tropical cyclone-like vortices (TCLVs) generated by a GCM simulation of the current climate were rerun for five days using a much higher-resolution regional model (Kurihara et al. 1998), and the resulting intensities compared to 51 cases simulated under enhanced greenhouse conditions. The forecast cases were initialized not with the weak vortices as detected in the GCM, but rather with a more realistic vortex that was artificially inserted (or ''bogussed'') into the initial fields. After five days of simulation, the intensity evolution of the two sets of 51 cases were compared. In general, the TCLVs were more intense by 5%–12% under enhanced greenhouse conditions, as measured by surface wind speed. This corresponded to a decrease in central surface pressure of 7–20 hPa. Applying a test of statistical significance to these results showed that they were only statistically significant at some times during the 5-day period of simulation. A similar result was shown for the most intense storms in the sample. The more recent study of Knutson and Tuleya (1999) generally supported these conclusions.

Knutson et al. (1998) also compared the simulated intensity changes under enhanced greenhouse conditions to those expected from the theoretical thermodynamic estimates of Emanuel (1988, 1995) and Holland (1997), and found that these estimates were comparable to the model results. All of this analysis was performed for a region of the northwest Pacific, where the model simulation was best and where historically the strongest typhoons are observed to occur.

Corresponding author address: Kevin Walsh, CSIRO Atmospheric Research, PMB1, Aspendale, Victoria, 3195, Australia.
E-mail: kevin.walsh@dar.csiro.au

We wish to explore this effect in another basin where the tropical cyclone climatology is different. Further, it is unknown whether the results of Knutson et al. (1998) are substantially model dependent. If a similar result were obtained in a different region of the globe using a different model, then more confidence could be placed in the results of Knutson et al. (1998) as a prediction of global change science.

This paper examines the same question as Knutson et al. (1998) but for the Australian region and using a different modeling system. This study uses a similar but independently developed methodology (Suppiah et al. 1996, 1998) to examine the question of whether the mean and maximum intensity of tropical cyclones are likely to change under enhanced greenhouse conditions.

Section 2 gives details of the model used and the experimental methodology, section 3 discusses the results, while section 4 provides some brief conclusions.

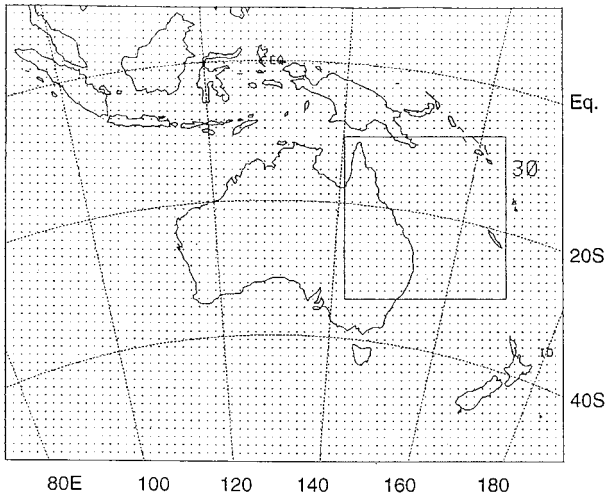

FIG. 1. Base domain of 125-km resolution with typical multiply nested 30-km domain indicated.

2. Model and methodology

The modeling system used here is based upon the regional climate model DARLAM (Division of Atmospheric Research Limited Area Model) developed at the Commonwealth Scientific and Industrial Research Organisation (CSIRO). The model is a two-time-level, semi-implicit, hydrostatic primitive equations model; it uses an Arakawa staggered C grid on a Lambert conformal projection, and semi-Lagrangian horizontal advection with bicubic spatial interpolation. In the present experiments, the model uses one-way nesting with lateral boundary conditions specified from the Mark 2 CSIRO 9-level R21 GCM (Watterson et al. 1997). This is an ''equilibrium'' model simulation in which both $1 \times CO_2$ and $2 \times CO_2$ runs are performed for fixed concentrations of CO_2 (330 and 660 ppm, respectively). An earlier version of DARLAM was more fully described in McGregor et al. (1993). Here, 20-yr seasonally varying simulations were performed for both models for the current climate ($1 \times CO_2$) and enhanced greenhouse conditions ($2 \times CO_2$). The CO_2 concentrations were changed in both models. In the GCM, SSTs were computed using a mixed layer model with implied ocean heat transports, that is, a *q*-flux correction (e.g., Hansen et al. 1984). Both models simulate the diurnal variation.

The simulations analyzed here are based upon those of McGregor and Katzfey (1997). There are some differences in regional climate model (RCM) formulation from that used in the earlier study of Walsh and Witterson (1997, hereafter WW97), which examined the ability of DARLAM to generate a realistic climatological distribution of TCLVs. An improved representation of surface vegetation has been included in the RCM (Kowalczyk et al. 1991). In this study, the RCM uses a convective parameterization which is the same as that in the forcing GCM, a modified Arakawa (1972) convection scheme. The method employed to force the RCM at its edges is also different from that used in WW97. Here, an exponential weighting of the GCM fields similar to that suggested by Giorgi et al. (1994) is included. The main effect of this technique, as compared to the earlier Davies (1976) scheme, is that anomalous concentrations of rainfall near the boundary of the RCM are generally removed.

Additionally, when simulations of the daily variability of the RCM in the Tropics were evaluated, it was found that tropical systems in the RCM tended to persist unrealistically if the relatively large domain used in simulations like these was only forced at its edges. Accordingly, a weak large-scale forcing from the GCM was implemented across the entire domain of DARLAM, in addition to the boundary forcing described above. At each time step of DARLAM, a gridbox average of 1400 km on a side of both DARLAM and the GCM fields of temperature, winds, and surface pressure was computed. The DARLAM box average was then relaxed back to the GCM box average every time step with a relaxation time of 96 h. Since only the box average was nudged, the smaller-scale features were relatively unaffected. This was found to substantially improve the simulation of tropical rainfall variability, while not significantly affecting the ability of DARLAM to generate intense storms. This forcing was not applied in the high-resolution (30 km) simulations described below because of their relatively short duration.

Two sets of DARLAM simulations were performed, a lower-resolution DARLAM run nested within the GCM and higher-resolution simulations nested within the lower-resolution DARLAM run. The lower-resolution or ''base'' DARLAM simulations were performed at a horizontal resolution of 125 km with nine vertical levels; the domain size is 70×57 (Fig. 1). Numerous TCLVs were detected in these simulations using the method described in WW97, which was adapted from that of Bengtsson et al. (1995). However, their inten-

sities compared to those of observed tropical cyclones were lower, as shown in WW97. Once these were detected at this lower resolution, a new, higher-resolution domain was nested with the base model simulation, and the TCLV was simulated for five days at the higher resolution. The boundary conditions for the higher-resolution simulations were taken from the base model DARLAM simulation. The higher-resolution domain comprised a horizontal resolution of 30 km and a vertical resolution of 18 levels. A fixed-mesh higher-resolution domain was used, and the TCLVs were inserted centered in the *x* direction but towards the north end of the grid to allow for the southward drift of almost all storms after initialization. As in Knutson et al. (1998), the vortex in the RCM was replaced by a more realistic bogussed vortex before the high-resolution simulations commenced, using the technique of Davidson et al. (1993). The original vortex detected in the RCM was blended with an idealized vortex with central pressure of 980 hPa, with most of the weighting in the blending procedure applied to the idealized vortex, and with only some contribution from the original vortex. The vortex thus created by the blending procedure was then initialized into the 30-km resolution simulation. Thus, the intensities of the initial vortices in all of the high-resolution simulations were similar. This rough equality of initial intensities has the advantage of reducing the large scatter of observed and simulated tropical cyclone intensities and thus increasing the likelihood that a statistically significant signal would emerge given the limited sample size of the study. In order to eliminate weaker vortices whose characteristics might be less like those of real tropical cyclones, a minimum strength threshold for detection in the base simulation was applied. This was a strength of 6 m s^{-1}, as measured by the Outer Core Wind Strength (OCS, Weatherford and Gray 1988a). For 1 × CO_2 conditions, 46 storms were simulated, while 50 were simulated under 2 × CO_2 conditions.

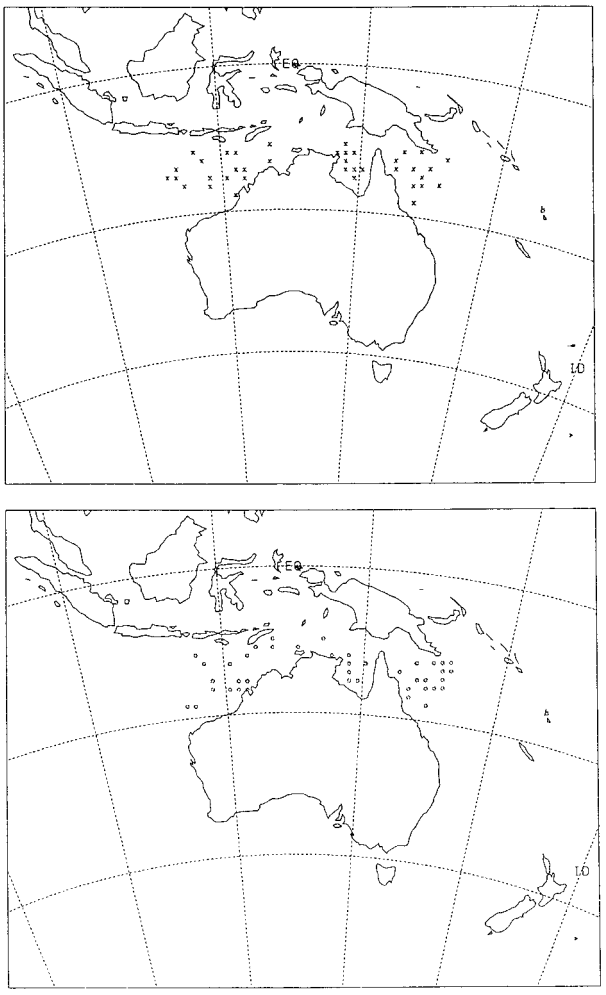

FIG. 2. Initial positions of bogussed vortices for (top) 1 × CO_2 conditions and (bottom) 2 × CO_2 conditions. Positions in (top) are marked by crosses and in (bottom) by circles.

3. Results

Figure 2 shows the initial positions of the bogussed vortices, which tend to be toward the center of the base domain. This is a result of the requirement that the 30-km resolution multiply nested grid be located entirely within the base domain and that the initial low be centered in the *x* direction. Figure 3 shows the radial-average structure of a typical TCLV at the time of its maximum intensity. As in observed tropical cyclones (Frank 1977), in the simulation shown in Fig. 3 the maximum radial-average tangential wind speed occurs some distance from the center of the storm at a height of about 850 hPa. This is accompanied by a maximum temperature anomaly near the center of the TCLV at a height of about 300 hPa, also as observed.

A comparison has been made of the distribution of simulated TCLV maximum wind speeds to observed tropical cyclone intensities in the Australian region. A random sample of 50 observed tropical cyclones was found to contain many more weak vortices (central pressures greater than 980 hPa) than simulated here. This is no doubt because of the specification of a relatively strong initial vortex (980 hPa) in the current experiments. The maximum intensities of the strongest tropical cyclones in the observed sample tended to be only slightly higher than the strongest of those simulated here under 1 × CO_2 conditions (not shown). This suggests that a reasonable distribution of intensity is obtained in the current simulations.

Figure 4 shows a comparison of simulated central pressures of TCLVs for 1 × CO_2 and 2 × CO_2 conditions, while Fig. 5 shows the same comparison for low-level wind speeds. The figures show mean values for all of the simulated TCLVs, as well as the standard deviations of their intensities at each day after initialization. The results indicate that there is an increase in

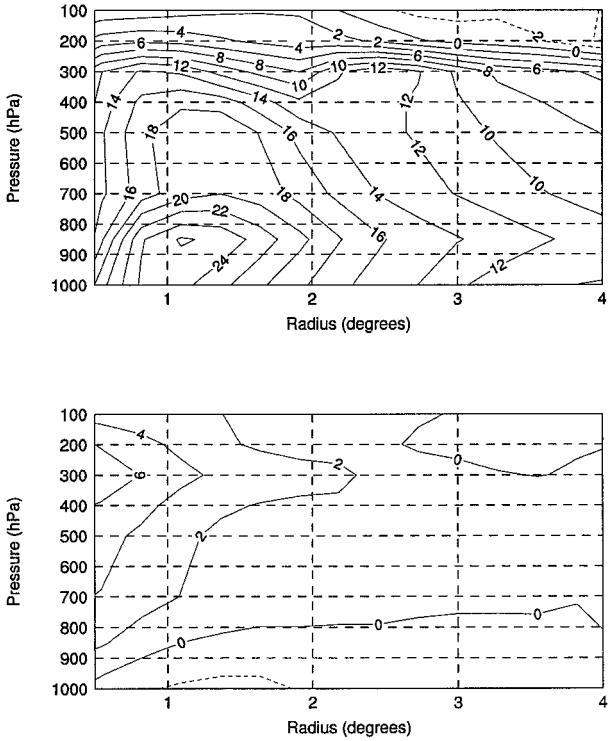

FIG. 3. Radial-average structure of a typical TCLV at time of maximum intensity: (top) tangential wind speed and (bottom) temperature anomaly. Contour interval is 2 m s^{-1} for (top), 2K for (bottom).

mean intensity under $2 \times CO_2$ conditions. The standard deviations of the intensities are quite large compared to the intensity increases, however, which suggests that the statistical significance of the differences is not large. To assess the significance of the differences in the distributions of pressures, the Kolmogorov–Smirnoff distribution test was applied. Those for day 1 are significant at the 95% level, but not for any other day. For the wind speeds, those for day 2 are significant at the 95% level, but not for any other days. The difference in storm intensities is larger than in the original 125-km resolution simulation, however, where there was little or no difference in intensity between $1 \times CO_2$ and $2 \times CO_2$ simulated intensities (not shown).

The standard deviations are larger in $2 \times CO_2$ conditions than in $1 \times CO_2$. This is caused by an increase in the number of stronger storms that is not entirely compensated for by a decrease in the number of weaker storms, in other words, the distribution of intensities becomes more skewed. This also reduced the statistical significance of the results.

Because many of the storms are initialized close to land, we have also calculated the intensity differences for only those TCLVs that do not strike land. Since storms that do not strike land suffer less from interactions with land surfaces that may tend to decrease their intensities, the intensity increases for storms that do not strike land are slightly larger than for storms that do

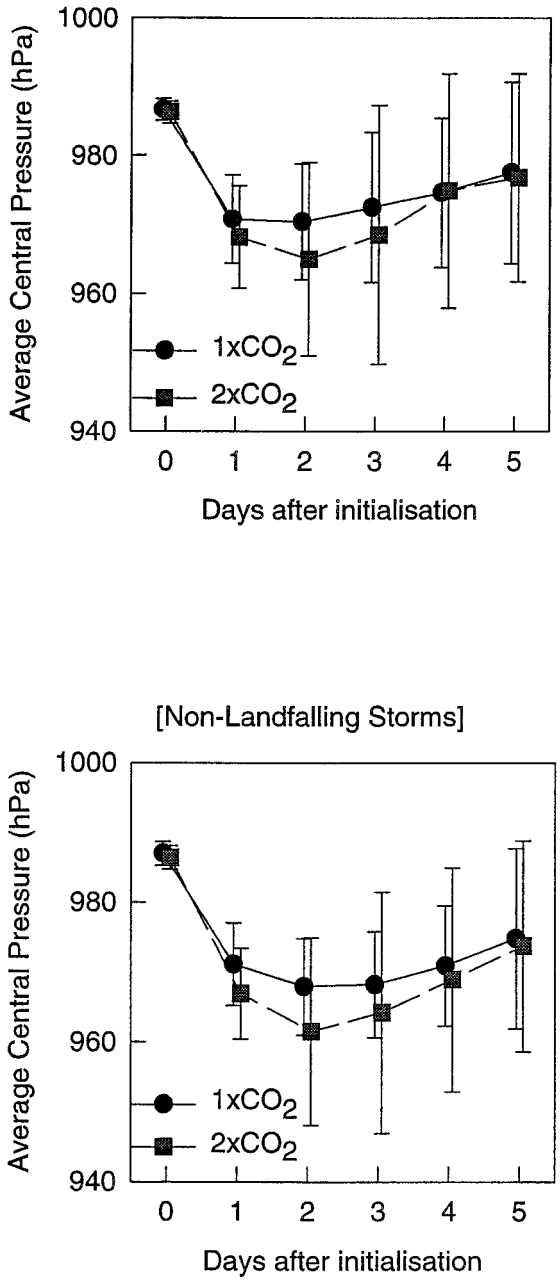

FIG. 4. Simulated mean central pressures of TCLVs for each day after initialization with standard deviations indicated by error bars for (top) all storms and (bottom) only storms that do not strike land.

(Figs. 4 and 5). Nevertheless, for wind speeds of storms that do not strike land, only the differences for day 2 are again statistically significant.

It is clear from Fig. 5 that increases in maximum intensity for storms might be more pronounced than the increases in the mean. Accordingly, to test this hypothesis, the maximum intensity reached by each TCLV was calculated and the distribution of these intensities for both experiments was compared. The results (Fig. 6) show a clear increase in the maximum intensities

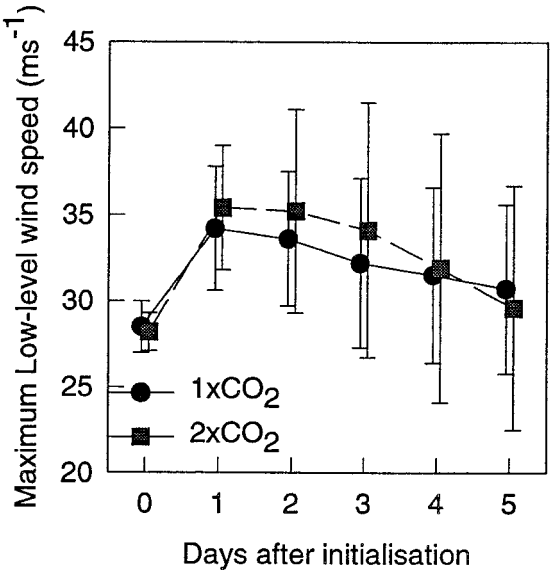

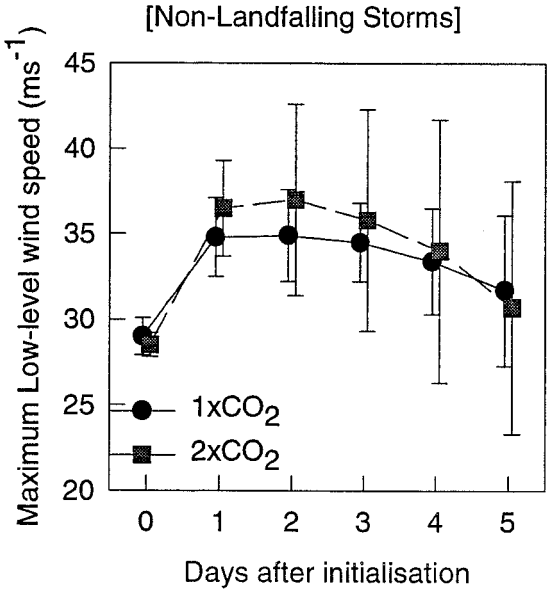

FIG. 5. The same as in Fig. 4 but for low-level wind speed.

reached by all TCLVs. Figure 7 shows the same results for minimum pressures. In neither case, though, were the distribution differences statistically significant, as measured by the chi-square test. Using the more sensitive Kolmogorov–Smirnoff test, the differences in the distributions of the maximum wind speeds were found to be significant at the 90% level, but not the minimum pressures. This level of statistical significance is very similar to the results found by Knutson et al. (1998; p. 1019).

In their study over the northwest Pacific region, Knut-

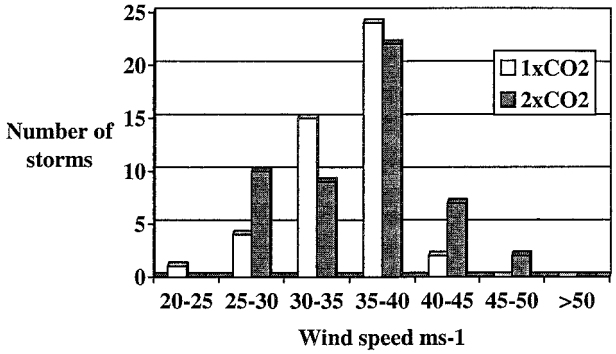

FIG. 6. Frequency of maximum wind speeds reached by TCLVs for (unshaded bars) $1 \times CO_2$ conditions conditions and (shaded bars) $2 \times CO_2$ conditions.

son et al. (1998) compared the simulated increases in intensities to theoretical calculations of MPI (Holland 1997; Emanuel 1988, 1995) as derived from the climatology of the host GCM. Measures of MPI use information about the thermodynamic structure of the atmosphere to calculate the amount of energy available in the atmosphere for tropical cyclone intensification. Knutson et al. (1998) found reasonable quantitative agreement between the theoretical predictions of intensity increase and the simulated increase in their modeling study. For comparison to theoretical estimates of MPI, the mean of the most intense 10% of TCLVs in the simulations presented here is calculated. In this way, any bias that might be present by only examining the most intense storm that happens to be simulated in this study may be partially removed. Therefore the mean of the minimum pressures of the five most intense storms in $1 \times CO_2$ and $2 \times CO_2$ conditions is calculated.

The mean of these five storms under $1 \times CO_2$ conditions is 953.8 hPa, and under $2 \times CO_2$ is 938 hPa. In terms of wind speeds, this represents an increase of about 13%. Both these pressure values are less than expected from the MPI diagnosed using Holland's (1997) formulation (see Fig. 8a for $1 \times CO_2$). Figure 8b shows that the theoretically expected MPI increase as diagnosed from the climatology of the base DAR-

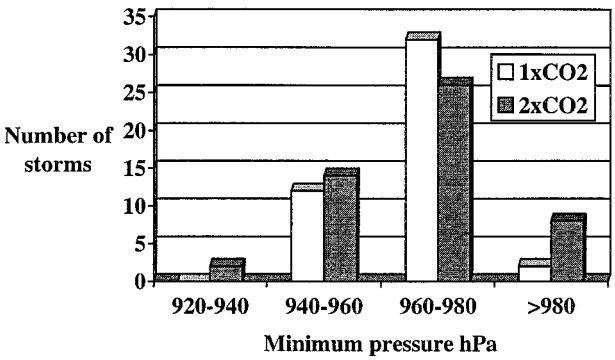

FIG. 7. The same as in Fig. 6 but for minimum central pressures.

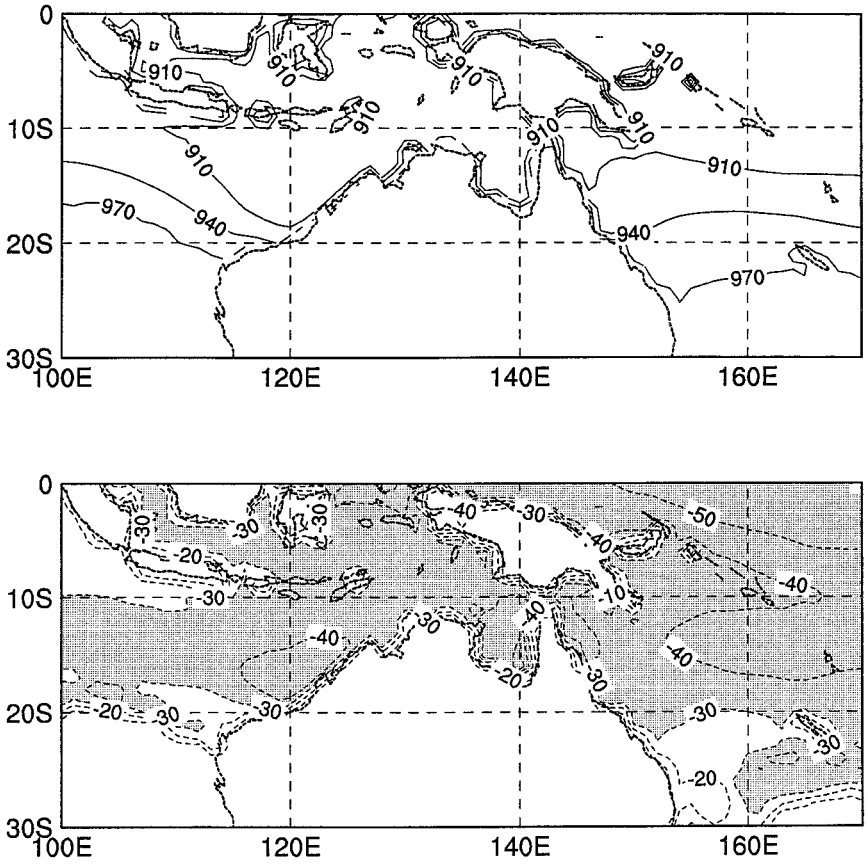

FIG. 8. Maximum potential intensity as diagnosed by Holland's (1997) technique from DARLAM for (top) $1 \times CO_2$ and (bottom) $2 \times CO_2$ minus $1 \times CO_2$ conditions. Contour interval is 30 hPa for (top), 10 hPa for (bottom). Differences larger than 30 hPa are shaded in (b).

LAM simulation is about 20–40 hPa over the simulated region. In terms of wind speeds, this corresponds roughly to an increase of 15%–25%, larger than the simulated increase. The change in MPI is diagnosed from an SST increase of 3°–4°C simulated by the mixed layer ocean model; SST increases for $2 \times CO_2$ conditions generated by coupled ocean–atmosphere GCMs are typically smaller than this (e.g., Gordon and O'Farrell 1997), and hence the present study may have overestimated the MPI response.

The fact that the simulated TCLVs are not reaching the predicted MPI may be caused by two factors. The horizontal resolution of the DARLAM simulations in this experiment is reasonable, but with higher resolution greater intensities would be simulated. In addition, the presence of vertical wind shear in the DARLAM simulations limits the ability of the storms to reach their MPI. We have illustrated the thermodynamic and dynamic influences limiting MPI by the following analysis. We compare the simulated maximum intensity reached to the vertical wind shear around the storm and the underlying SST at the time of maximum intensity, for nonlandfalling storms only. The vertical wind shear is determined by calculating the mean wind vectors at 850 and 200 hPa in a square of 40 grid points (about 1200 km) on a side centered on the storm center. The first 48 h of simulation were excluded, since intensities of storms during this period almost always increased uniformly irrespective of the environmental conditions as the initialized storm adjusted to its surroundings.

Figure 9 shows the maximum intensity reached as a function of the vertical wind shear and the SST at that time and location. The results indicate both a tendency for intensities to be greater with less wind shear and greater with higher SSTs, although this is not a perfect correspondence. The relationship between shear and maximum intensity is better for higher SSTs than for lower, which is also the case under $2 \times CO_2$ conditions (not shown). This suggests that episodes of high vertical wind shear have a more important effect in limiting storm intensities when the ocean is warm, that is, at lower latitudes. This is in agreement with theoretical and observational studies (DeMaria 1996). A multiple regression analysis in which the wind shear and SST were used to predict the maximum intensity gave a substantial relationship, with the variance explained $r^2 = 0.42$, a result above the 95% significance level. A less strong but similarly statistically significant result was

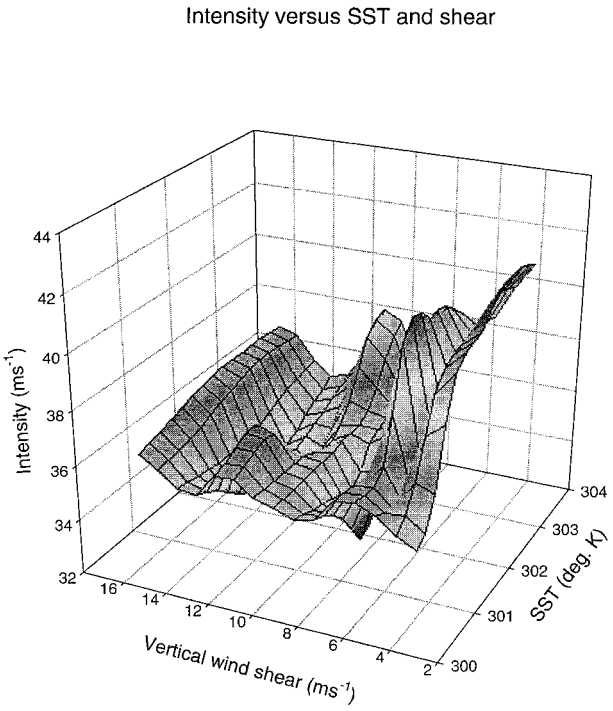

FIG. 9. Maximum intensity of TCLVs as a function of vertical wind shear and SST under $1 \times CO_2$ conditions.

found for $2 \times CO_2$ conditions ($r^2 = 0.33$). Under $1 \times CO_2$ conditions, a reasonable result was also obtained from correlating SST and maximum intensity alone, but the percentage of variance explained was much lower with $r^2 = 0.17$ ($r = 0.41$). This result suggests that although there is some relationship between maximum intensity and thermodynamic constraints as indicated by SST, a much better relationship is obtained when dynamic constraints are also introduced. Similarly, for $2 \times CO_2$ conditions the percentage variance explained by SST alone was also slightly lower than for the multiple regression at $r^2 = 0.28$ ($r = 0.53$).

Similarly, when shear is correlated with intensity normalized by MPI, a reasonably strong inverse relationship was found for $1 \times CO_2$ ($r = -0.49$). This suggests that vertical wind shear, as expected, is limiting the ability of the simulated TCLVs to approach their MPI. One implication of this is that a limited sample of simulations such as those presented here would not necessarily simulate the maximum possible intensity, even if the horizontal resolution were higher. This effect would be most pronounced in regions with high climatological wind shear. A weaker relationship was found for correlation between maximum intensity and shear alone ($r = -0.35$). However, little relationship between shear and intensity normalized by MPI was found under $2 \times CO_2$ conditions ($r = -0.09$). Analysis showed that this poor correlation was largely due to one storm that reached a high intensity despite high wind shear under conditions of high SST. The correlation between maximum intensity and shear alone was similar ($r = -0.13$) for the same reason.

4. Conclusions

Idealized tropical cyclones are inserted into a high-resolution regional climate model and their subsequent intensity evolution examined under current and enhanced greenhouse conditions. It is found that, in agreement with previous work and theoretical considerations, intensities under enhanced greenhouse conditions are slightly greater, although the differences are generally not statistically significant. The differences in maximum intensities reached by each storm are larger than the differences averaged over each day of simulation, and larger for storms that do not strike land compared to all storms. For storms that do not strike land, the strongest simulated storms do not reach the theoretically derived maximum potential intensity. One cause could be the limited resolution of the regional climate model. Another could be that dynamical influences such as vertical wind shear, which are not included in theoretical estimates of maximum potential intensity, act to restrict the development of the storm and thereby its maximum intensity. It is suggested that these dynamical effects probably will be greatest in regions of high climatological wind shear.

Acknowledgments. The authors thank John McGregor and Kim Nguyen for work on the development of DARLAM and the simulations analyzed in this paper. We would like to thank Jack Katzfey and Barrie Hunt for some useful comments. We gratefully acknowledge the financial support of the governments of the Northern Territory, Western Australia and Queensland, and of CSIRO.

REFERENCES

Arakawa, A., 1972: Design of the UCLA general circulation model. Numerical simulation of weather and climate. Tech. Rep. 7, Dept. of Meteorology, University of California, Los Angeles, 116 pp. [Available from Department of Atmospheric Sciences, University of California, Los Angeles, CA 90024-1565.]

Bengtsson, L., M. Botzet, and M. Esch, 1995: Hurricane-type vortices in a general circulation model. *Tellus,* **47A,** 175–196.

Davidson, N. E., J. Wadsley, K. Puri, K. Kurihara, and M. Ueno, 1993: Implementation of the JMA typhoon bogus in the BMRC tropical prediction system. *J. Meteor. Soc. Japan,* **71,** 437–467.

Davies, H. C., 1976: A lateral boundary formulation for multi-level prediction models. *Quart. J. Roy. Meteor. Soc.,* **102,** 405–418.

DeMaria, M., 1996: The effect of vertical wind shear on tropical cyclone intensity change. *J. Atmos. Sci.,* **53,** 2076–2087.

Emanuel, K. A., 1988: The maximum intensity of hurricanes. *J. Atmos. Sci.,* **45,** 1143–1155.

——, 1995: Sensitivity of tropical cyclones to surface exchange coefficients and a revised steady-state model incorporating eye dynamics. *J. Atmos. Sci.,* **52,** 3969–3976.

Frank, W. M., 1977: The structure and energetics of the tropical cyclone. I. Storm structure. *Mon. Wea. Rev.,* **105,** 1119–1135.

Giorgi, F., C. S. Brodeur, and G. T. Bates, 1994: Regional climate

change scenarios over the United States produced with a nested regional climate model. *J. Climate*, **7,** 375–399.

Gordon, H. B., and S. P. O'Farrell, 1997: Transient climate change in the CSIRO coupled model with dynamic sea ice. *Mon. Wea. Rev.*, **125,** 875–907.

Hansen, J., A. Lacis, D. Rind, G. Russell, P. Stone, I. Fung, R. Ruedy, and J. Lerner, 1984: Climate sensitivity: Analysis of feedback mechanisms. *Climate Processes in Meteorology*, J. E. Hansen and T. Takahashi, Eds., Amer. Geophys. Union, 130–163.

Henderson-Sellers, A., and Coauthors, 1998: Tropical cyclones and global climate change: A post–IPCC assessment. *Bull. Amer. Meteor. Soc.*, **79,** 19–38.

Holland, G. J., 1997: The maximum potential intensity of tropical cyclones. *J. Atmos. Sci.*, **54,** 2519–2541.

Knutson, T. R., and R. E. Tuleya, 1999: Increased hurricane intensities with CO_2-induced warming as simulated using the GFDL hurricane prediction system. *Climate Dyn.*, **15,** 503–519.

——, ——, and Y. Kurihara, 1998: Simulated increase of hurricane intensities in a CO_2-warmed world. *Science*, **279,** 1018–1020.

Kowalczyk, E. A., J. R. Garratt, and P. B. Krummel, 1991: A soil-canopy scheme for use in a numerical model of the atmosphere–1D stand-alone model. CSIRO Division of Atmospheric Research, Tech. Paper 23, 59 pp. [Available from CSIRO Atmospheric Research, PMB 1, Aspendale, Vic. 3195, Australia.]

Kurihara, Y., R. E. Tuleya, and M. A. Bender, 1998: The GFDL hurricane prediction system and its performance in the 1995 hurricane season. *Mon. Wea. Rev.*, **126,** 1306–1322.

Li, S., 1996: Estimating tropical cyclone intensity from climate models. M. S. thesis, Climatic Impacts Centre, Macquarie University, Sydney, Australia, 136 pp. [Available from Department of Physical Geography, Division of Environmental and Life Science, Macquarie University, NSW 2109, Australia.]

McGregor, J. L., and J. J. Katzfey, 1997: Climate modelling for the Australian region using DARLAM. *Proc. Int. Workshop on General Monsoon System*, Beijing, China, START Regional Centre for Temperate East Asia, 13–18.

——, H. B. Gordon, I. G. Watterson, M. R. Dix, and L. D. Rotstayn, 1993: The CSIRO 9-level atmospheric general circulation model. CSIRO Division of Atmospheric Research, Tech. Paper 26, 89 pp. [Available from CSIRO Atmospheric Research, PMB 1, Aspendale, Vic. 3195, Australia.]

Suppiah, R., R. J. Allan, K. J. Hennessy, R. N. Jones, A. B. Pittock, K. J. E. Walsh, I. N. Smith, and P. H. Whetton, 1996: Climate change under enhanced greenhouse conditions in northern Australia: Second annual report 1995–1996. CSIRO Division of Atmospheric Research, 63 pp. [Available from CSIRO Atmospheric Research, PMB 1, Aspendale, Vic. 3195, Australia.]

——, and Coauthors, 1998: Climate change under enhanced greenhouse conditions in northern Australia: Third annual report 1996–1997. CSIRO Division of Atmospheric Research, 95 pp. [Available from CSIRO Atmospheric Research, PMB 1, Aspendale, Vic. 3195, Australia.]

Walsh, K., and I. G. Watterson, 1997: Tropical cyclone-like vortices in a limited area model: Comparison with observed climatology. *J. Climate*, **10,** 2240–2259.

Watterson, I. G., S. P. O'Farrell, and M. R. Dix, 1997: Energy and water transport in climates simulated by a general circulation model that includes dynamic sea ice. *J. Geophys. Res.*, **102,** 11 027–11 037.

Weatherford, C. L., and W. M. Gray, 1988: Typhoon structure as revealed by aircraft reconnaisance. Part I: Data analysis and climatology. *Mon. Wea. Rev.*, **116,** 1032–1043.